

## Geophysical Investigation of Some Flood Prone Areas in Ota, Southwestern Nigeria

*A.P. Aizebeokhai, O.M. Alile, J.S. Kayode and F.C. Okonkwo*

Department of Physics, CST, Covenant University, Canaan Land, Ota, Ogun State, Nigeria

---

**Abstract:** Thirteen shallow vertical electrical resistivity soundings using Schlumberger array were conducted within the study area. The aim of the study was to investigate the nature of the subsurface in some flood prone areas within the study area by determining the lithology and the corresponding inverse model resistivities at the depths investigated and hence the cause of flooding in the area during the wet season. The resistivity sounding data were collected along seven traverses using a Campus Tigre terrameter. The observed data were interpreted quantitatively using curve matching and computer assisted iteration method. The results of the inversion show a lithology that comprises of the top soil and a paralic sequence of sand and lateritic clay at the depth investigated with varied resistivity and thickness. The flooding is thought to be due to the shallow lateritic clay layer at an average depth of 5.2 m with thickness ranging from 14.5m to 31.8m at the various points of investigation and the shallow depth of the water table.

**Key words:** Geophysical investigation • Electrical resistivity • Soundings • Flood prone areas • Ota

---

### INTRODUCTION

Electrical resistivity methods of prospecting are more diversified than many other geophysical methods. Some of the methods such as self potential and telluric currents depend on naturally occurring fields as in magnetic and gravity prospecting, while others depend on artificial fields as in seismic techniques. Electrical resistivity surveying involves the detection of surface effects produced by electric currents flowing in the ground and it is affected by clay contents, groundwater conductivity, soil or formation porosity and degree of water saturation.

A wide variety of electrical surveying techniques exist unlike most geophysical surveying methods where a single field of force or anomalous property such as gravity, elasticity, magnetism and radioactivity is used. In electrical methods of prospecting, potentials, currents, electromagnetic fields, which may occur naturally or be introduced artificially in the earth may be measured. The measurements can be made in a variety of ways to determine a variety of results. It is the variation in electrical conductivity (or resistivity) found in different rocks and minerals that makes electrical methods possible.

Geophysical resistivity techniques are based on the response of subsurface materials to the flow of electric currents. In these methods, an electric current is injected

into the ground and two potential electrodes are used to measure the resulting potential difference between the current electrodes and thus allowing for the measurement of the electrical impedance of the subsurface materials. Apparent resistivity is a function of the measured impedance (ratio of potential to current) and the geometry of the electrode array. Depending upon the survey geometry, the apparent resistivity data are plotted as 1-D soundings, 1-D profiles, or in 2-D cross-sections in order to look for anomalous regions.

In the shallow subsurface, the presence of water controls much of the conductivity variations. In general, the measurement of resistivity is a measure of the water saturation and connectivity of pore space. Increasing saturation, salinity of the underground water, porosity of rocks (water-filled voids) and the degree of fractures or weathering tend to decrease the subsurface resistivity. Increasing compaction of soils or rock units will expel water and will effectively increase resistivity. Air, which naturally has high resistivity, results in the opposite response compared to water when filling voids. Whereas the presence of water will reduce resistivity, the presence of air in voids should increase subsurface resistivity [1].

This survey was conducted in areas prone to flooding during the wet season in some parts of Ota. The nature of the subsurface layers in these constantly flooded areas have not been previously investigated.

Thus, the study was carried to ascertain the cause of the flooding by investigating the nature of the subsurface geometry and aquifers. This would help to understand the nature of the geomaterials and their permeability or porosity, as well as pore structures and hence the groundwater potential of the sites investigated.

**Geology of Study Area:** The study area is located in the eastern Dahomey basin of the southwestern Nigeria. The Dahomey basin forms one of a series of West African Atlantic Margin basins that were initiated during the period of rifting in the late Jurassic to early Cretaceous, [2-4]. The basin stretches along the coast of Nigeria, Benin Republic, Togo and Ghana along the margin of the Gulf of Guinea (Fig. 1, [5]). It is separated from the Niger Delta in the Eastern section by the Benin Hinge Line and Okitipupa Ridge and marks the continental extension of the chain fracture zone [6, 7]. It is bounded on the west by the Ghana Ridge and has been interpreted as the Romanche fracture zone [8, 4].

The stratigraphy of the Cretaceous and Tertiary Formations in the Nigerian section of the basin is controversial. This is due primarily to different stratigraphic names that have been proposed for the same Formation in different localities in the basin [9, 10]. This situation can be partly blamed on the lack of good borehole coverage and adequate outcrops for detailed stratigraphic studies. Earlier studies on the basin stratigraphy by Jones and Hockey [11] recognized both

Cretaceous and Tertiary sediments (Figs. 1 and 2, [5]). Other, subsequent workers recognized three chronostratigraphic units: pre-lower Cretaceous folded sequence, Cretaceous sequence and Tertiary sequence [2, 9]. The Cretaceous stratigraphy as compiled from outcrop and borehole records consists of the Abeokuta Group, sub-divided into three formational units, namely Ise, Afowo and Araromi [2]. The Tertiary sediments comprise the Ewekoro, Akinbo, Oshosun, Ilaro and Benin Formations (Fig. 2).

The Abeokuta Group is mainly composed of poorly sorted ferruginized grit, siltstone and mudstone with shale-clay layers [12]. The Group is partly marine, brackish and fresh water in origin; it thickens and then continues into Dahomey. The Abeokuta Group is overlain by the Ewekoro Formation and then the Akinbo Formation both of which are of the Paleocene age [13]. Akinbo Formation is the upper beds of shale that overlies the limestone and this could be of the lowermost Eocene age. The shales were however accorded formational status as the shale overlying the Ewekoro limestone [14]. The top of the formation is marked by pure grey gritty sand and then little clay. The Akinbo Formation passes gradationally into massive mud and is overlain by the Oshosun Formation, which is usually marine and of the Eocene age. The Oshosun Formation is overlain by a sequence of predominantly coarse sandy estuarine, deltaic and continental beds which display rapid lateral facies changes and it is named the Illaro formation.

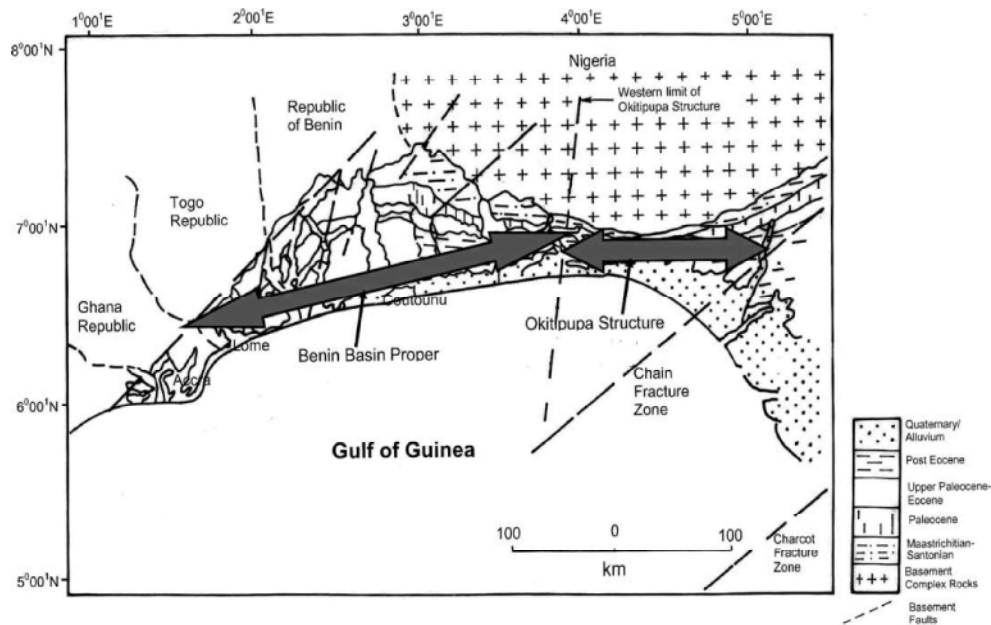


Fig. 1: Simplified regional map of Dahomey basin; the Nigeria part show both Cretaceous and Tertiary rocks (after [5])

AGE		GROUP	FORMATIONS
QUATERNARY			
TERTIARY	PLIOCENE		ILARO
	MIOCENE		
	OLIGOCENE		
	EOCENE		
	PALEOCENE		
CRETACEOUS	MAASTRICHTIAN		ARAROMI
	CAMPANIAN		
	SANTONIAN		
	CONIACIAN		
	TURONIAN		
	CENOMANIAN		
	ALBIAN		
	APTIAN		
	BARREMIAN		
	NEOCOMIAN		
		ISE	OKITIPUPA RIDGE (BASEMENT)
		AFOWO	

Fig. 2: Simplified Cretaceous and Tertiary stratigraphy of Nigeria part of Dahomey Basin (after [5])

The sandy Abeokuta Group is underlain by the basement complex and harbours aquifer zone which is unattractive since it cannot be considered as good prospect for groundwater exploration because of the impending low yield capacity. The Ewekoro Formation also bears similar aquifer characteristics and but the Akinbo Formation has been found to be a good source of groundwater exploration. The structural features that occur within the basement rocks are due to tectonic activities and they include: joints, faults and fractures.

**Theory of Resistivity Surveying:** A brief summary of resistivity theory is presented here. Essentially, the basis of all resistivity sounding is a differential equation in electric potential that reduces to Laplace's equation for isotropic media. Hence, particular solution for electric potential and apparent resistivity may be derived for a number of model representations of the earth. The most common model is a horizontally stratified earth of homogenous and isotropic layers. A review is given of theoretical approaches to the forward problem of calculating sounding curves over such a model.

The inverse problem of converting field measurements into a geoelectric section is invariably solved in terms of an earth model of horizontal layers. Sometimes, however, a field sounding suggests departures from such a simple model and allowances, usually qualitative, may be made during interpretation. Traditional methods of qualitative interpretation are examined and are shown to be outdated; emphasis is placed on computer based methods of analysis. Mailliet [15], expounded the fundamental theory behind the resistivity method and the theory has been adequately covered by Keller and Frischknecht [16], Grant and West [17] and Bhattacharyya and Partra [18].

The dielectric and magnetic properties of earth materials may be expressed in terms of the Maxwell's equation as:

$$\nabla \times \underline{H} = \underline{J} + \frac{\partial \underline{D}}{\partial t} \tag{1}$$

$$\nabla \times \underline{E} = -\frac{\partial \underline{B}}{\partial t} \tag{2}$$

$$\nabla \cdot \underline{B} = 0 \tag{3}$$

$$\nabla \cdot \underline{D} = Q \tag{4}$$

The vector  $\underline{H}$  and  $\underline{B}$  are the magnetic field strength and magnetic flux density, whereas the vectors  $\underline{E}$  and  $\underline{D}$  are the electric field strength and electric displacement, respectively, the quantity  $Q$  is the electric charge density and  $\underline{J}$  is the current density. The equation of continuity of current may be obtained by taken the divergence of equation (1), so that

$$\nabla \cdot \nabla \times \underline{H} = \nabla \cdot \underline{J} + \nabla \cdot \frac{\partial \underline{D}}{\partial t} \tag{5}$$

$$\Rightarrow \nabla \cdot \underline{J} = -\frac{\partial}{\partial t} \nabla \cdot \underline{D} \tag{6}$$

Since the divergence of the curl of a vector is zero and the derivative with respect space coordinates and time can be reversed. From equations (4) and (6), we have that

$$\nabla \cdot \underline{J} = -\frac{\partial Q}{\partial t} \tag{7}$$

The resistivity method operates in the absence of a field of induction and is based on observations of an electric field maintained by direct current. However, for source free regions of the earth, equations (2) and (7) become  $\nabla \times \underline{E} = 0$  and  $\nabla \cdot \underline{J} = 0$ .

However, Ohm's law provides the relationship between electric field strength  $\underline{E}$  and the current density  $\underline{J}$  such that the current is proportional to the electric field, the constant of proportionality,  $\sigma$  being the conductivity of the material.

$$\underline{J} = \sigma \underline{E} \quad (8)$$

The electric field strength may be expressed as the gradient of a scalar potential,  $V$  so that  $\underline{E} = -\nabla V$ . For an isotropic medium, the conductivity will be a scalar quantity so that the vectors  $\underline{J}$  and  $\underline{E}$  will be in the same direction. In general,  $\underline{J}$  and  $\underline{E}$  are not in the same direction because might be easier in one direction. Such a medium is said to be isotropic and the conductivity is a tensor of second rank with subscripts  $i$  and  $j$  which may be any of the  $x$ ,  $y$  and  $z$  spatial directions in a rectangular coordinate system. Thus, Ohm's law becomes  $\underline{J} = \underline{\sigma} \underline{E}$ , or more fully

$$\begin{bmatrix} J_x \\ J_y \\ J_z \end{bmatrix} = \begin{bmatrix} \sigma_{xx} & \sigma_{xy} & \sigma_{xz} \\ \sigma_{yx} & \sigma_{yy} & \sigma_{yz} \\ \sigma_{zx} & \sigma_{zy} & \sigma_{zz} \end{bmatrix} \begin{bmatrix} E_x \\ E_y \\ E_z \end{bmatrix}$$

Thus, the differential equation that forms the basis of all resistivity prospecting with direct current may be expressed as  $\nabla \sigma_{ij} \nabla V = 0$ . In isotropic case where the conductivity at a point in the ground is independent of direction, equation (10) reduces to Laplace's equation  $\nabla^2 V = 0$ . The solution to these equations may be developed for a particular model of the earth by selecting a coordinate system to match the geometry of the model and imposing appropriate boundary conditions.

**Methodology:** Thirteen vertical electrical resistivity soundings (VES) were conducted in the study area using Schlumberger arrays. The include a Campus Tigre terrameter was used for the apparent resistivity measurements. The area is a gently sloping plain with a maximum elevation difference of about 7m. Since the

targets of interest are at shallow depths, a maximum current electrode spacing (AB/2) of 100 m was used in survey. The terrameter was set on a cycle of 5 so that the resistivity meter can sample the subsurface resistance 5 times before finally displaying the median of the measurements. The current used by the terrameter varied between 5mA and 10mA and it supplied a voltage of 12.6V during this survey. The RMS errors in the measurements were generally less than 2% and the measurements were repeated for isolated cases in which the RMS errors were higher than this. The terrameter was set on resistance and the apparent resistivities were obtained by multiplying the observed resistance with the geometric factor which was calculated based on the electrode spacing for each data point. The observed apparent resistivities are given in Table 1(a-d).

Conventional curve matching technique was used in the preliminary interpretation of the thirteen VES data obtained from the locations in the study area. Curve matching technique, which involves a comparison of the measured apparent resistivity curve with a set of theoretically calculated master curves, is traditionally used in interpreting VES data obtained over horizontal stratification. The observed apparent resistivity values were plotted against the current electrode spacing (AB/2) using transparent paper on a log-log graph. This graph was then superimposed on mathematically calculated Schlumberger master curves for vertical electrical resistivity soundings for preliminary interpretations of the layer model resistivity values and thicknesses.

The results obtained from the curve matching were then used as input data for the resistivity inversion on a fast digital computer. The WinResist computer software was used to carry out the inversion. During the inversion, the apparent resistivity values obtained during the survey were first plotted against the current electrode spacing (AB/2) by the software, then the preliminary results for the inverse model resistivity values of the layer models with their corresponding thickness obtained from the curve matching were used as input data for the inversion proper. An iteration process was conducted until a good curve fitting was obtained between the field curves and computed curves. The root mean square (RMS) errors of less than 5% were generally obtained; however, root mean square errors up to 5% are considered satisfactory.

Table 1(a-d): Tables showing the apparent resistivity results obtained in the study areas

AB/2m	MN/2m	GeometricFactor [K]	VES 1		VES 2		VES 3	
			R <sub>1</sub> [Ω]	KR <sub>1</sub> [Ωm]	R <sub>2</sub> [Ω]	KR <sub>2</sub> [Ωm]	R <sub>3</sub> [Ω]	KR <sub>3</sub> [Ωm]
1.0	0.25	6.28	63.14	396.519	63.40	398.152	37.26	233.993
1.3	0.25	10.62	45.80	486.396	40.54	430.535	25.44	270.173
1.8	0.25	20.36	28.98	590.033	20.10	409.236	12.50	254.500
2.4	0.25	36.19	19.32	699.191	10.87	393.385	7.548	273.162
3.2	0.25	64.34	10.78	693.585	5.504	354.127	4.278	275.247
4.2	0.25	110.85	6.315	700.018	2.950	327.008	2.795	309.826
4.2	1.0	27.71	34.33	951.284	14.23	394.313	15.44	427.842
5.5	1.0	47.52	19.84	942.797	8.488	403.350	9.23	438.610
7.5	1.0	88.36	6.514	575.577	4.770	421.477	4.875	430.755
10	1.0	157.08	3.796	596.276	3.079	483.649	2.898	455.218
13	1.0	265.47	2.433	645.889	2.104	558.549	1.544	409.886
13	2.5	106.19	6.168	654.980	4.443	471.802	3.822	405.858
18	2.5	203.60	3.614	735.810	2.838	577.819	1.803	367.091
24	2.5	361.91	2.570	930.109	2.122	767.973	1.276	461.797
32	2.5	643.40	1.854	1192.864	1.604	1032.014	0.862	554.611
42	2.5	1108.35	1.302	1443.072	1.034	1146.034	0.5599	620.565
55	2.5	1900.66	0.8023	1524.900	0.5659	1075.583	0.3779	718.259
55	5.0	950.33	1.613	1532.882	1.104	1094.164	0.974	925.621
75	5.0	1767.16	0.8386	1481.940	0.4288	757.758	0.7609	1344.632
100	5.0	3141.59	0.3502	1100.185	0.2079	653.137	0.502	1577.078

Table 1b

AB/2m	MN/2m	GeometricFactor [K]	VES 4		VES 5		VES 6	
			R <sub>4</sub> [Ω]	KR <sub>4</sub> [Ωm]	R <sub>5</sub> [Ω]	KR <sub>5</sub> [Ωm]	R <sub>6</sub> [Ω]	KR <sub>6</sub> [Ωm]
1.0	0.25	6.28	105.2	660.656	54.00	339.120	22.77	142.996
1.3	0.25	10.62	63.49	674.264	22.51	239.056	11.21	119.050
1.8	0.25	20.36	29.67	604.081	7.68	156.365	5.763	117.335
2.4	0.25	36.19	16.04	580.488	4.081	147.691	3.589	129.886
3.2	0.25	64.34	8.273	532.285	2.286	147.081	2.174	139.875
4.2	0.25	110.85	4.434	491.509	1.665	184.565	1.440	159.624
4.2	1.0	27.71	23.63	654.787	5.495	152.266	5.944	164.708
5.5	1.0	47.52	12.94	614.909	3.873	184.045	4.098	194.737
7.5	1.0	88.36	7.013	619.669	2.613	230.885	2.717	240.074
10	1.0	157.08	4.348	682.984	1.716	269.549	1.803	283.215
13	1.0	265.47	2.622	696.062	1.156	306.883	1.268	336.616
13	2.5	106.19	6.013	638.520	2.528	268.448	3.192	338.958
18	2.5	203.60	3.657	744.565	1.518	309.065	1.984	403.942
24	2.5	361.91	2.191	792.945	1.018	368.424	1.328	480.616
32	2.5	643.40	1.207	776.584	0.6401	411.840	0.888	571.339
42	2.5	1108.35	0.6987	774.404	0.3692	409.203	0.5849	648.274
55	2.5	1900.66	0.3209	609.922	0.1699	322.922	0.3718	706.665
55	5.0	950.33	0.6712	637.861	0.358	340.218	0.7678	729.663
75	5.0	1767.16	0.3002	530.501			0.3364	594.473
100	5.0	3141.59						

Table 1c

AB/2m	MN/2m	GeometricFactor [K]	VES 7		VES 8		VES 9	
			R <sub>7</sub> [Ω]	KR <sub>7</sub> [Ωm]	R <sub>8</sub> [Ω]	KR <sub>8</sub> [Ωm]	R <sub>9</sub> [Ω]	KR <sub>9</sub> [Ωm]
1.0	0.25	6.28	101.7	638.676	38.21	239.959	67.89	426.349
1.3	0.25	10.62	56.59	600.986	22.94	243.623	30.79	326.990
1.8	0.25	20.36	32.61	663.940	12.25	249.410	17.94	365.258
2.4	0.25	36.19	17.34	627.535	7.264	262.884	10.52	380.719
3.2	0.25	64.34	8.265	531.770	4.460	286.956	5.461	351.361
4.2	0.25	110.85	4.71	522.104	2.735	303.175	3.062	339.423
4.2	1.0	27.71	26.39	731.267	11.38	315.340	12.94	358.567
5.5	1.0	47.52	15.61	741.787	7.790	370.181	7.635	362.815
7.5	1.0	88.36	8.032	709.708	6.211	548.804	4.365	385.691
10	1.0	157.08	4.262	669.475	5.253	825.141	2.942	462.129
13	1.0	265.47	2.614	693.939	3.088	819.771	2.122	563.327
13	2.5	106.19	7.135	757.666	8.455	897.836	6.470	687.049
18	2.5	203.60	3.727	758.817	2.924	595.326	3.839	781.620
24	2.5	361.91	2.260	817.917	1.760	636.962	2.268	820.812
32	2.5	643.40	1.578	1015.285	1.095	704.523	1.337	860.226
42	2.5	1108.35	0.905	1003.057	0.7204	798.455	0.7773	861.520
55	2.5	1900.66	0.5504	1046.123	0.4227	803.409	0.4728	898.632
55	5.0	950.33	1.061	1008.300	0.8205	779.746	1.078	1024.456
75	5.0	1767.16	0.3856	681.417	0.3890	687.425	0.5288	934.474
100	5.0	3141.59	0.2286	718.167	0.1639	514.907	0.2294	720.681

Table 1d

AB/2m	MN/2m	GeometricFactor [K]	VES 10		VES 11		VES 12		VES 13	
			R <sub>10</sub> [Ω]	KR <sub>10</sub> [Ωm]	R <sub>11</sub> [Ω]	KR <sub>11</sub> [Ωm]	R <sub>12</sub> [Ω]	KR <sub>12</sub> [Ωm]	R <sub>13</sub> [Ω]	KR <sub>13</sub> [Ωm]
1.0	0.25	6.28	172.5	1083.300	179.4	1126.632	73.07	458.880	70.22	440.982
1.3	0.25	10.62	87.9	933.498	108.7	1154.394	49.08	521.223	42.53	451.669
1.8	0.25	20.36	45.20	920.272	52.45	1067.882	22.43	456.675	21.91	446.088
2.4	0.25	36.19	23.79	860.960	27.69	1002.101	10.52	380.719	13.45	486.756
3.2	0.25	64.34	12.76	820.978	14.83	954.162	6.816	438.541	7.936	510.602
4.2	0.25	110.85	7.005	776.504	7.591	841.462	3.779	418.902	4.503	499.158
4.2	1.0	27.71	27.77	769.507	32.17	891.431	23.46	650.077	20.18	559.188
5.5	1.0	47.52	16.56	786.931	16.39	778.853	11.99	569.765	10.95	520.344
7.5	1.0	88.36	7.678	678.428	7.60	671.536	6.134	542.000	5.590	493.932
10	1.0	157.08	4.253	668.061	4.209	661.150	3.494	548.838	2.976	467.470
13	1.0	265.47	2.691	714.380	2.691	714.380	2.139	567.840	1.829	485.545
13	2.5	106.19	6.738	715.508	6.642	705.314	5.823	618.344	5.590	593.602
18	2.5	203.60	3.433	698.959	4.098	834.353	3.175	646.430	3.071	625.256
24	2.5	361.91	1.984	718.029	2.433	880.527	1.924	696.315	1.906	689.800
32	2.5	643.40	1.207	776.584	1.389	893.683	1.104	710.314	1.225	788.165
42	2.5	1108.35	0.7955	881.692	0.7687	851.989	0.6013	666.451	0.5711	632.979
55	2.5	1900.66	0.4434	842.753	0.4331	823.176	0.3209	609.922	0.2803	532.755
55	5.0	950.33	0.8326	791.245	0.923	877.155	0.7600	722.251	0.4952	470.603
75	5.0	1767.16	0.3580	632.643	0.4606	813.954	0.3951	698.205	0.1924	340.002
100	5.0	3141.59	0.1104	346.832	0.2130	669.159	0.1457	457.730	0.0616	193.522

**RESULTS AND DISCUSSION**

The results obtained from the preliminary interpretation of the field data provided initial estimates of the resistivity and thickness values of the subsurface formations and served as starting models for the inversion using a fast digital computer. The results obtained from the inversion of the apparent resistivity values are shown in Figs. 3 to 15. The RMS error values are all below 5%, except in VES 8 where the RMS error value is 5.8% and this is because the data for this VES point were very noisy. Table 2(a-d) shows the layer models, their true resistivities, thicknesses and depths obtained from the results of the inversion of the observed apparent resistivity values. The tables show a correlation in the resistivities, thicknesses and depths of the layers along each traverse.

VES 1, 2, 3, were carried out along traverse one. The results obtained from the interpretation of the field data showed that three lithologic units, comprising of the top most soil, sand and clay were probed. The thickness of the layers along this traverse is between 0.5m and 17.9m and the resistivity is between 200.2Ωm and 5770.3Ωm. The main aquifers are located between 13.3m and 23.4m. VES 4 was carried out along traverse two. The results obtained from the inversion of the data gotten at this point showed that there are three lithologic units here, comprising of top most soil, sand and clay. The thickness of the layers range between 1.5m and 15.8m and their resistivities are between 426.5Ωm and 1263.5Ωm. The main aquifer is located at a depth of 20.6m.

VES 5 was carried out along traverse three. There are three lithologic units at this point comprising of the top most soil, sand and clay. The layers have thicknesses between 0.4m and 14.5m, while their resistivities range

between 116.8Ωm and 702.9Ωm. The main aquifer can be found at a depth of 17.8m. VES 6 was carried out along traverse four. There are three lithologic units made up of the overburden, clay and sand, at this point. The overburden comprises of the top most soil and sand and it has a thickness of 3.3m and a resistivity of 123.6Ωm, while the clay has a thickness of 31.8m and a resistivity of 976.9Ωm. The main aquifer is located at a depth of 35.1m.

VES 7, 8, 9, were carried out along traverse five. The result obtained from the inversion of the data gotten along this traverse shows that the depth investigated is made up of seven layers comprising of top most soil, dry sand, porous sand, dry clay and wet clay. The thicknesses of the layers along this traverse are between 0.4m and 12.8m and their resistivities range between 206.0Ωm and 2375.8Ωm. The main aquifers are located between 21.4m and 25.3m. The inversion of VES 8 had an rms error of 5.8% and this is due to the noisy data obtained on the field at the location where this VES was carried out.

VES 10, 11, 12, were carried out along traverse six. The area generally consists of eight layers, although the data interpretation of VES 10 showed that there are seven layers at that point. The layers along this traverse comprises of the top most soil, dry sand, porous sand and lateritic clay. The thicknesses of the layers along this traverse range between 0.5m and 14.2m and their resistivity values are between 102.2Ωm and 1907.4Ωm. The main aquifers can be found between 23.8m and 43.3m. VES 13 was carried out along traverse seven. The results obtained from the inversion of the data observed at this location shows that there are five layers comprising of the top most soil, sand and lateritic clay. The thicknesses of the layers here are between 1.2m and 11.9m, while their resistivities range between 79.9Ωm and 1638.1Ωm.

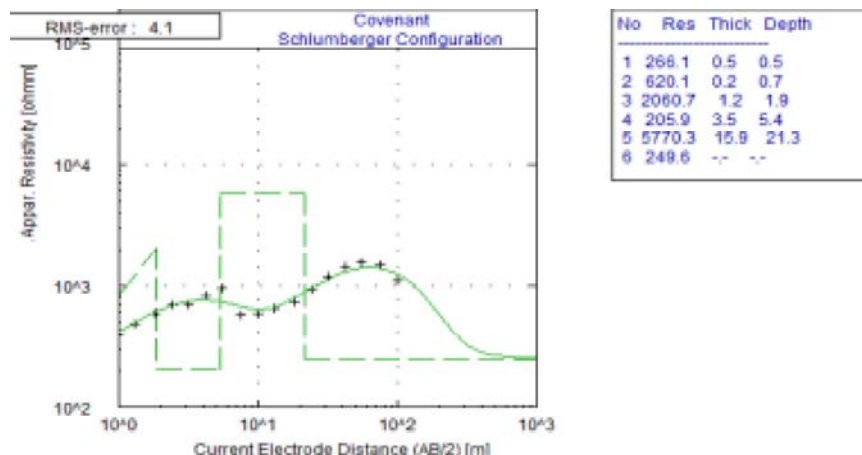


Fig. 3: Inverse model of VES 1

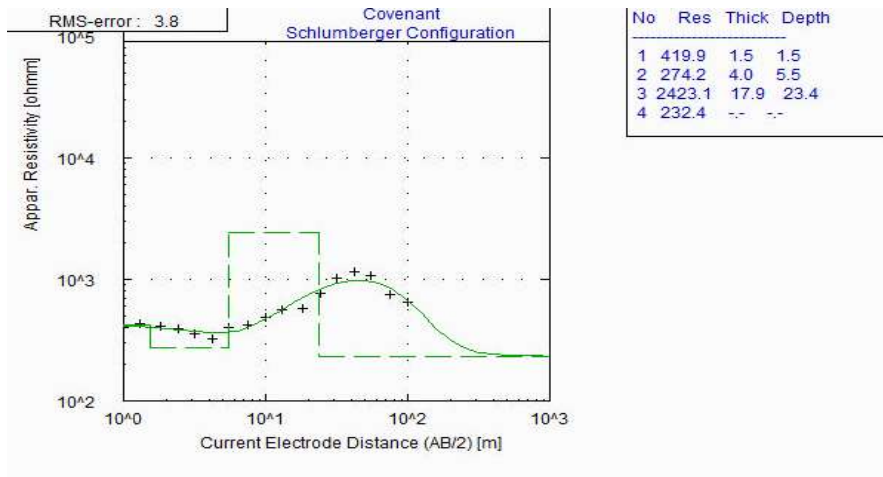


Fig 4: Inverse model of VES 2

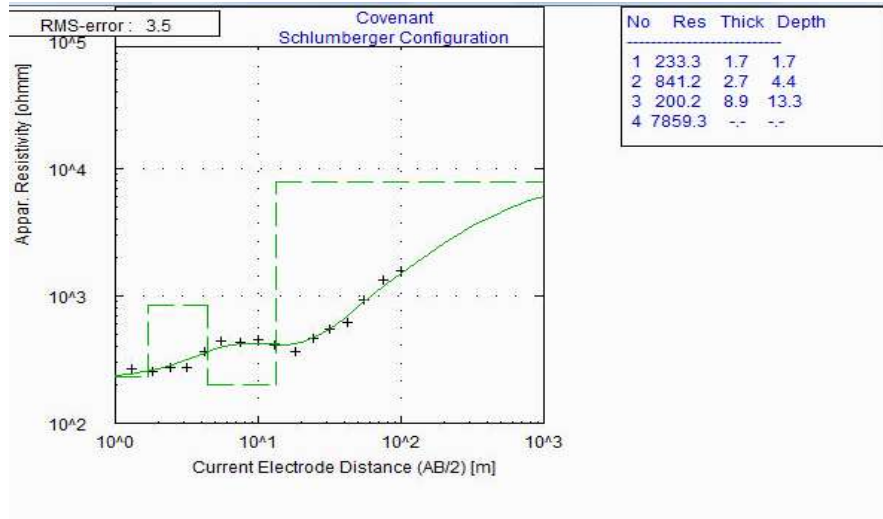


Fig 5: Inverse model of VES 3

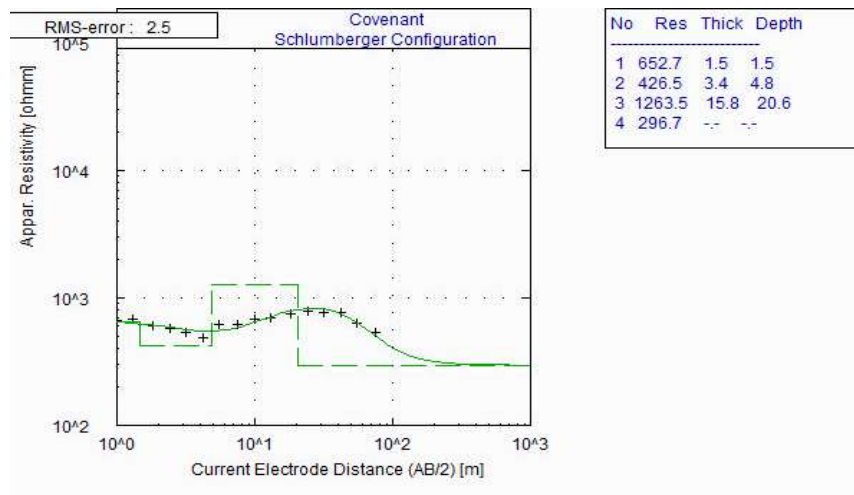


Fig 6: Inverse model of VES 4

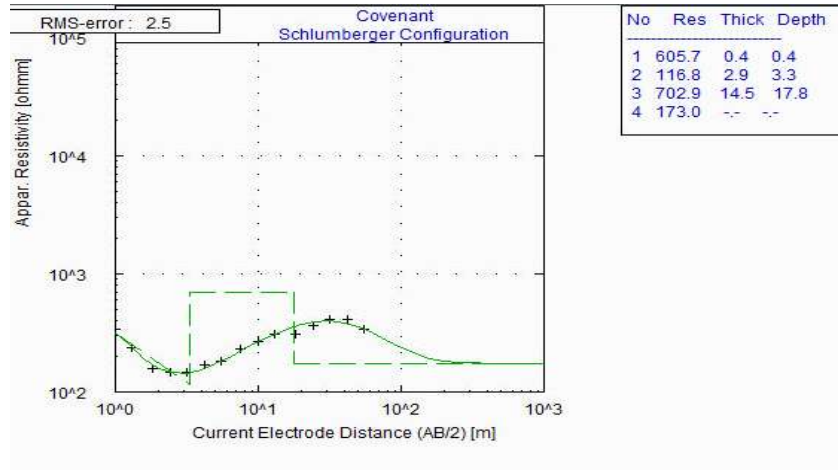


Fig 7: Inverse model of VES 5

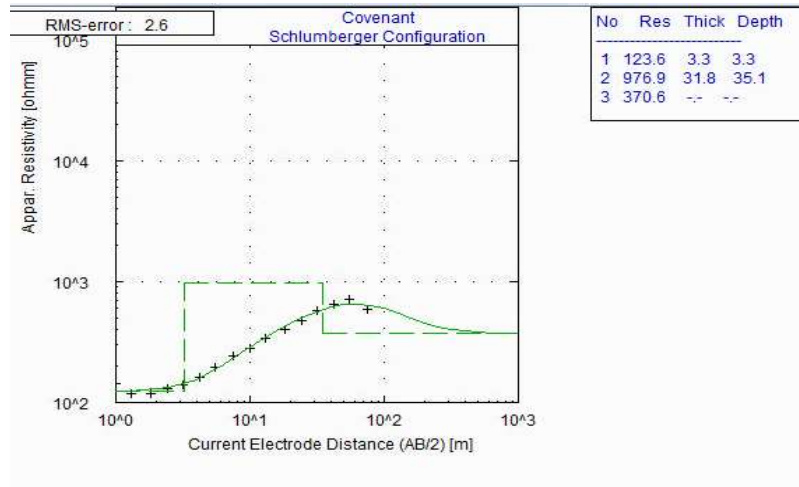


Fig 8: Inverse model of VES 6

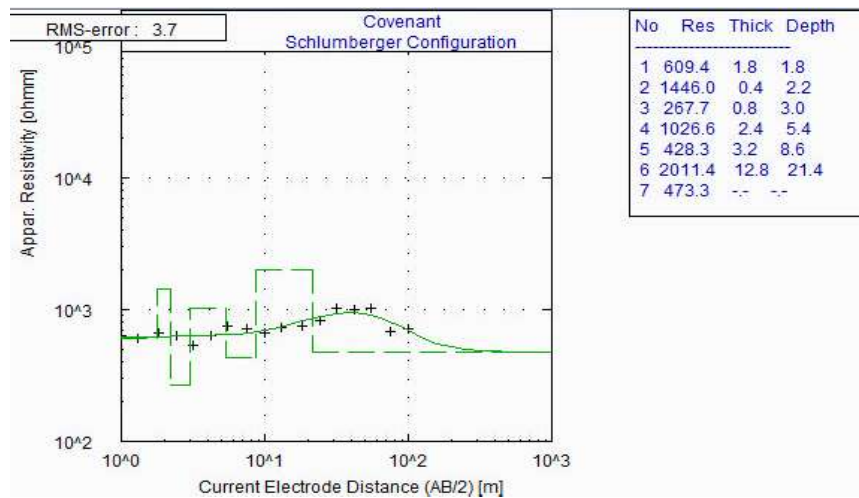


Fig 9: Inverse model of VES 7

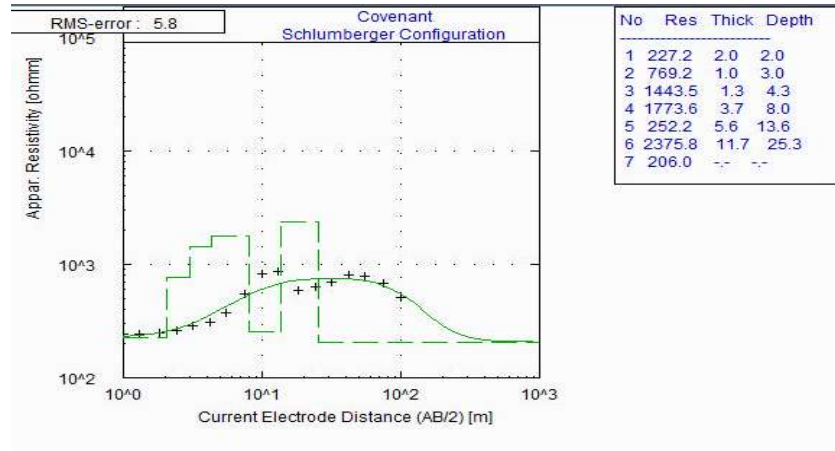


Fig. 10: Inverse model of VES 8

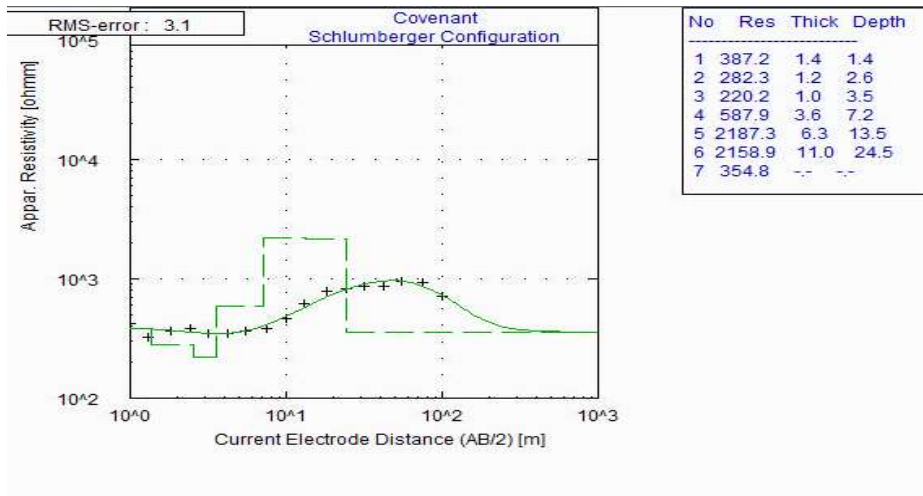


Fig. 11: Inverse model of VES 9

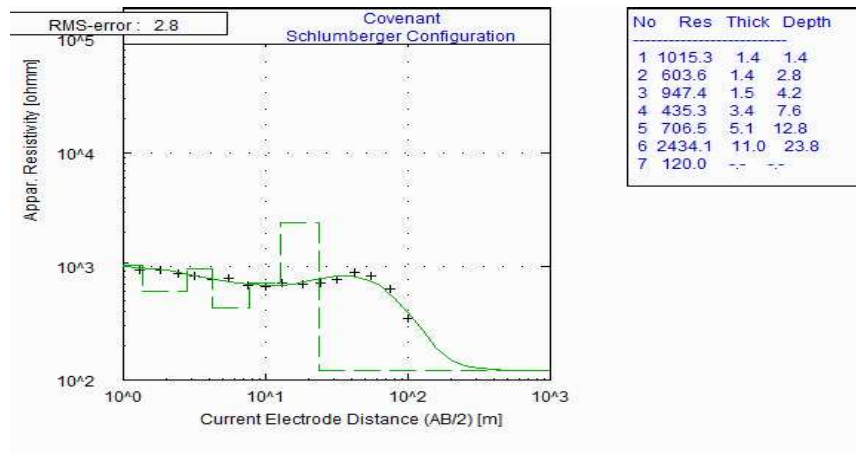


Fig. 12: Inverse model of VES 10

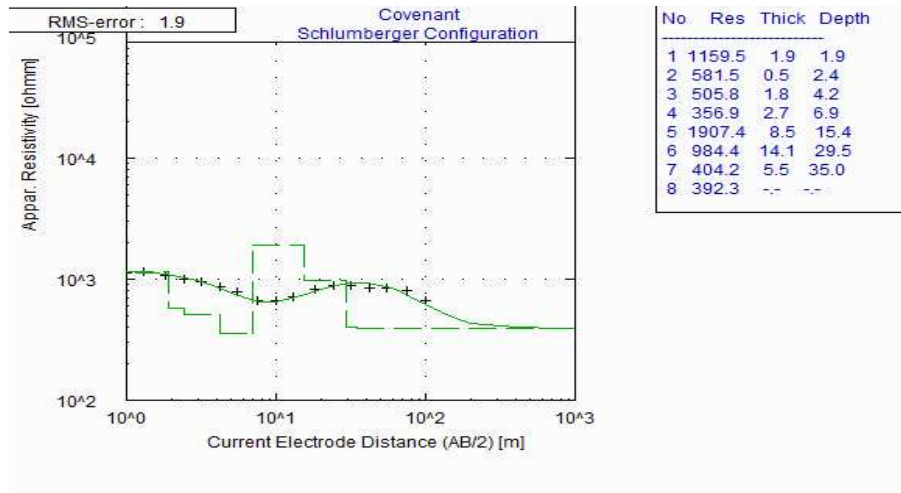


Fig. 13: Inverse model of VES 11

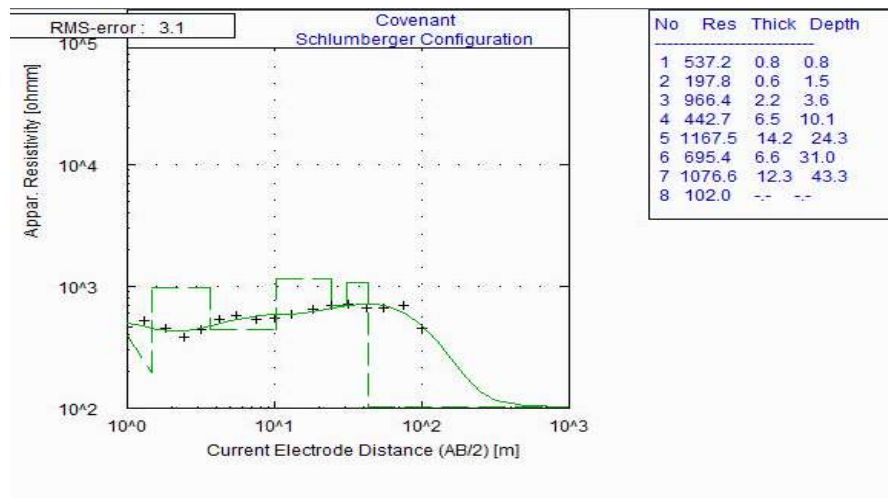


Fig. 14: Inverse model of VES 12

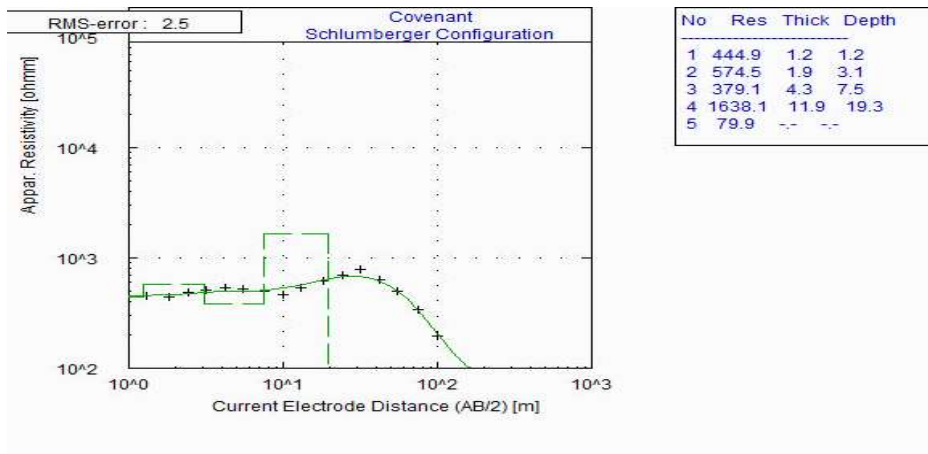


Fig. 15: Inverse model of VES 13

Table 2(a-d): Model resistivity values for layer models

Table 2a

	Possible lithology	Top most soil	Lateritic clay	Sand	Lateritic clay	Sand	
VES 1	Resistivity ( $\Omega\text{m}$ )	266.1	620.1	2060.7	205.9	5770.3	249.6
	Thickness (m)	0.5	0.2	1.2	3.5	15.9	-
	Depth (m)	0.5	0.7	1.9	5.4	21.3	-
VES 2	Resistivity ( $\Omega\text{m}$ )	419.9	-	-	274.2	2423.1	232.4
	Thickness (m)	1.5	-	-	4.0	17.9	-
	Depth (m)	1.5	-	-	5.5	23.4	-
VES 3	Resistivity ( $\Omega\text{m}$ )	233.3	-	841.2	200.2	7859.3	-
	Thickness (m)	1.7	-	2.7	8.9	-	-
	Depth (m)	1.7	-	4.4	13.9	-	-
VES 4	Resistivity ( $\Omega\text{m}$ )	652.7	-	-	426.5	1263.5	296.7
	Thickness (m)	1.5	-	-	3.4	15.8	-
	Depth (m)	1.5	-	-	4.8	20.6	-
VES 5	Resistivity ( $\Omega\text{m}$ )	605.7	-	-	116.8	702.9	173.0
	Thickness (m)	0.4	-	-	2.9	14.5	-
	Depth (m)	0.4	-	-	3.3	17.8	-
VES 6	Resistivity ( $\Omega\text{m}$ )	-	-	-	123.6	976.9	370.6
	Thickness (m)	-	-	-	3.3	31.8	-
	Depth (m)	-	-	-	3.3	35.1	-

Table 2b

LAYER MODELS										
	Possible Lithology	Top most soil	Sand	Lateritic clay	Sand	Lateritic clay	Sand	Lateritic clay	Lateritic clay	Sand
VES 7	Resistivity ( $\Omega\text{m}$ )	-	609.4	1446.0	267.7	1026.6	428.3	-	2011.4	473.3
	Thickness (m)	-	1.8	0.4	0.8	2.4	3.2	-	12.8	-
	Depth (m)	-	1.8	2.2	3.0	5.4	8.6	-	21.4	-
VES 8	Resistivity ( $\Omega\text{m}$ )	227.2	769.2	1443.5	-	1773.6	252.2	-	2375.8	206.0
	Thickness (m)	2.0	1.0	1.3	-	3.7	5.6	-	11.7	-
	Depth (m)	2.0	3.0	4.3	-	8.0	13.6	-	25.3	-
VES 9	Resistivity ( $\Omega\text{m}$ )	387.2	282.3	-	220.2	-	587.9	2187.3	2158.9	354.8
	Thickness (m)	1.4	1.2	-	1.0	-	3.6	6.3	11.0	-
	Depth (m)	1.4	2.6	-	3.5	-	7.2	13.5	24.5	-

Table 2c

LAYER MODELS											
		Top most soil	Sand	Lateritic clay	Sand	Lateritic clay	Lateritic clay	Sand	Sand	Lateritic clay	Sand
VES 10	Resistivity ( $\Omega\text{m}$ )	1015.3	603.6	947.4	435.3	706.5	2434.1	120.0	-	-	-
	Thickness (m)	1.4	1.4	1.5	3.4	5.1	11.0	-	-	-	-
	Depth (m)	1.4	2.8	4.2	7.6	12.8	23.8	-	-	-	-
VES 11	Resistivity ( $\Omega\text{m}$ )	1159.5	581.5	505.8	356.9	1907.4	984.4	404.2	392.3	-	-
	Thickness (m)	1.9	0.5	1.8	2.7	8.5	14.1	5.5	-	-	-
	Depth (m)	1.9	2.4	4.2	6.9	15.4	29.5	35.0	-	-	-
VES 12	Resistivity ( $\Omega\text{m}$ )	537.2	197.8	966.4	442.7	1167.5	-	695.4	1076.6	102.0	-
	Thickness (m)	0.8	0.6	2.2	6.5	14.2	-	6.6	12.3	-	-
	Depth (m)	0.8	1.5	3.6	10.1	24.3	-	31.0	43.3	-	-

Table 2d

LAYER MODELS						
	Possible Lithology	Top most soil	Sand	Sand	Lateritic clay	Sand
VES 13	Resistivity ( $\Omega\text{m}$ )	444.9	574.5	379.1	1638.1	79.9
	Thickness (m)	1.2	1.9	4.3	11.9	-
	Depth (m)	1.2	3.1	7.5	19.3	-

The main aquifer is located at a depth of 19.3m. The resistivities, thicknesses and depths of the layer models discussed above, are shown comprehensively in Table 1 to 4.

From the above analysis of the results obtained, three lithologic units namely the top soil, sand and lateritic clay, were delineated although these layers have different arrangements at different locations. The top most soil have thicknesses between 0.4m and 2.0m and resistivities ranging from 123.6 $\Omega$ m to 1159.5 $\Omega$ m. The sand layers have thicknesses between 0.6m and 8.9m and their corresponding resistivities range from 79.9 $\Omega$ m to 984.4 $\Omega$ m, while the lateritic clay have thicknesses between 0.4m and 31.8m and resistivities between a range of 404.2 $\Omega$ m and 5770.3 $\Omega$ m. A stream is located along the point where VES 13 was carried out and this is responsible for the very low resistivity (79.9 $\Omega$ m) that was observed there. The depth of the water table is shallow and the main aquifers in all the survey sites are generally located between depths of 13.3m and 43.3m. These layer models are presented as geoelectric sections below. The flooding is thought to be due to the shallow lateritic clay layer at an average depth of 5.2 m with thickness ranging from 14.5m to 31.8m at the various points of investigation and the shallow depth of the water table.

### CONCLUSION

Resistivity survey has been carried out on some flood prone areas Ota, around Covenant University campus, Southwestern Nigeria. The results obtained from the curve matching and inversion show that the area is a sedimentary terrain, made up of three lithologic units namely the top most soil and paralic sequence of sand and lateritic clay. The top most soil has a thickness between 0.4m and 2.0m and resistivity range of 123.6 $\Omega$ m to 1159.5 $\Omega$ m. The sand layers have thicknesses between 0.6m and 8.9m and their corresponding resistivities range between 79.9 $\Omega$ m and 984.4 $\Omega$ m, while the lateritic clay has a thickness between 0.4m and 31.8m and a resistivity range of 404.2 $\Omega$ m and 5770.3 $\Omega$ m. The main aquifers in all the survey sites are generally located between depths of 13.3m and 43.3m.

From the inversion, it was observed that the top most soil comprises of mud and the first few meters of the subsurface. The sand layers have relatively low resistivities as compared to the lateritic clay layers and this is due to the porous, permeable and transmissible nature of sand. So the sand absorbs water when it rains, but it allows this water to flow through it into deeper

layers in the subsurface because of its porous nature. The lateritic clay in the subsurface due to the compact nature of its pore is not permeable and not transmissible and thus has very high resistivity values. Therefore whenever it rains, it stores water but does not allow water to pass through it, so the water continues accumulating on top of it until the water gets to the surface and this causes flooding. Also, because the depth of the water table in these areas is shallow, it quickly gets filled up when it rains and this is another reason why flooding occurs in this area especially during the wet season.

### REFERENCES

1. Cardimona, S., 2002. Electrical resistivity techniques for subsurface investigations: [http://www.dot.ca.gov/hq/esc/geotech/gg/geophysics2002/061cardimona\\_resistivity\\_overview.pdf](http://www.dot.ca.gov/hq/esc/geotech/gg/geophysics2002/061cardimona_resistivity_overview.pdf).
2. Omatsola, M.E. and O.S. Adegoke, 1981. Tectonic evolution and Cretaceous stratigraphy of the Dahomey basin. *Nigeria J. Mining and Geol.*, 18(01): 130-137.
3. Weber, K.J. and E. Daukoru, 1975. Petroleum geology of the Niger Delta. Ninth World Petroleum Congress, 2: 209-221.
4. Whiteman, A., 1982. *Nigeria: Its Petroleum Geology, Resources and Potential*. Graham and Trotman, pp: 394.
5. Olabode, S.O., 2006. Siliciclastic slope deposits from the Cretaceous Abeokuta Group, Dahomey (Benin) Basin, southwestern Nigeria. *J. African Earth Sci.*, 46: 187-200.
6. Coker, S.J.L. and J.E. Ejedawe, 1987. Petroleum prospect of the Benin basin Nigeria. *J. Mining and Geol.*, 23(01): 27-43.
7. Onuoha, K.O., 1999. Structural features of Nigeria's coastal margin: an assessment based on age data from wells. *J. African Earth Sci.*, 29(03): 485-499.
8. Burke, K.C.B., T.F.J. Dessauvage and A.J. Whiteman, 1971. The opening of the Gulf of Guinea and the geological history of the Benue depression and Niger Delta. *Nature Physical Sci.*, 233(38): 51-55.
9. Billman, H.G., 1992. Offshore stratigraphy and paleontology of Dahomey (Benin) Embayment. *NAPE Bulletin*, 70(02): 121-130.
10. Coker, S.J.L., 2002. Field excursion guide to tar sand outcrops in Benin Basin. NAPE Mini- Conference, pp: 32.

11. Jones, H.A. and R.D. Hockey, R.D., 1964. The geology of part of southwestern Nigeria. Geological Survey of Nigeria (GSN) Bulletin 31: 101.
12. Kogbe, C.A., 1989. *Geology of Nigeria*. Rock View (Nig.) Ltd., Nigeria.
13. Adegoke, S.O., T.F.J. Dessauvage and A.J. Whiteman, 1970. Macrofauna of Ewekoro Formation (Paleocene) of S.W. Nigeria, (In) African Geology. University of Ibadan, pp: 269-276.
14. Ogbe, F.A.G., 1970. Stratigraphy of strata exposed in Ewekoro quarry western Nigeria (In) Africa geology (T.F.J. Dessauvage and A.J. Whiteman, Eds.), University of Ibadan, pp: 305-324.
15. Maillet, R., 1947. The Fundamental equations of electrical prospecting. *Geophysics*, 12(4): 529-556.
16. Keller, G.V. and F.C. Frischknecht, 1966. *Electrical Method in Geophysical Prospecting*. Pergamon, Oxford, pp: 517.
17. Grant, F.S. and O.F. West, 1965. *Interpretation theory of applied geophysics*. Mcgraw-Hill, New York, pp: 583.
18. Bhattacharya, P.K. and H.P. Partra, 1968. Direct current geoelectric sounding. Elseviert, Amsterdam, pp: 135.